Available online at www.sciencedirect.com
ScienceDirect
Ceramics International 37 (2011) 3557–3564
CERAMICS INTERNATIONAL
www.elsevier.com/locate/ceramint

Studies on ionic conductivity of stabilized zirconia ceramics (8YSZ) densified through conventional and non-conventional sintering methodologies

K. Rajeswari [a], M. Buchi Suresh [a], U.S. Hareesh [a], Y. Srinivasa Rao [a], Dibakar Das [b], Roy Johnson [a,*]

[a] Centre for Ceramic Processing, International Advanced Research Centre for Powder Metallurgy and New Materials, Hyderabad 500005, India
[b] School of Engineering Sciences and Technology, HCU, Hyderabad, India

Received 23 March 2011; accepted 24 May 2011
Available online 15 June 2011

Abstract

Densification studies of 8 mol% yttria stabilized zirconia ceramics were carried out by employing the sintering techniques of conventional ramp and hold (CRH), spark plasma sintering (SPS), microwave sintering (MWS) and two-stage sintering (TSS). Sintering parameters were optimized for the above techniques to achieve a sintered density of >99% TD. Microstructure evaluation and grain size analysis indicated substantial variation in grain sizes, ranging from 4.67 μm to 1.16 μm, based on the sintering methodologies employed. Further, sample was also sintered by SPS technique at 1425 °C and grains were intentionally grown to 8.8 μm in order to elucidate the effect of grain size on the ionic conductivity. Impedance spectroscopy was used to determine the grain and grain boundary conductivities of the above specimens in the temperature range of RT to 800 °C. Highest conductivity of 0.134 S/cm was exhibited by SPS sample having an average grain size of 1.16 μm and a decrease in conductivity to 0.104 S/cm was observed for SPS sample with a grain size of 8.8 μm. Ionic conductivity of all other samples sintered vide the techniques of TSS, CRH and MWS samples was found to be ∼0.09 S/cm. Highest conductivity irrespective of the grain size of SPS sintered samples, can be attributed to the low densification temperature of 1325 °C as compared to other sintering techniques which necessitated high temperatures of ∼1500 °C. The exposure to high temperatures while sintering with TSS, CRH and MWS resulted into yttria segregation leading to the depletion of yttria content in fully stabilized zirconia stoichiometry as evidenced by Energy Dispersive Spectroscopy (EDS) studies.

Keywords: A. Sintering; C. Impedance; C. Ionic conductivity; D. ZrO_2; D. Y_2O_3; E. Fuel cells

1. Introduction

Densification methodologies play a major role in developing ceramic components with full density and fine sintered grain sizes. As various sintering methodologies proceed through diverse mechanisms and densification kinetics, it is possible to engineer sintered ceramics with desired microstructure. The conventional ramp and hold sintering (CRH), employing longer durations of soaking time at peak temperatures often leads to abnormal grain growth. The two stage sintering (TSS) methodology, introduced recently by Chen and Wang, utilizes the principle that the activation energy for grain growth is lower than the activation energy of densification [1]. The non-conventional methodologies for sintering ceramics primarily comprise of microwave sintering (MW) and spark plasma sintering (SPS). Microwave sintering, in the presence of an electromagnetic field, exploits the tendency of a dielectric material to couple with the microwave resulting in the generation of heat within. The technique generally uses a frequency of 2.45 GHz resulting in relatively rapid heating rates leading to uniform grained microstructures. Spark plasma sintering simultaneously applies pulsed electrical current and pressure directly on the sample leading to densification at relatively lower temperatures and shorter retention times [2–7].

8-mol% yttria-stabilized zirconia (8YSZ) is widely chosen as the electrolyte in solid oxide fuel cells (SOFCs) because of its excellent high temperature ionic conductivity [8]. The ionic conductivity of the electrolyte is strongly related to the microstructure of the electrolyte material [9]. Gibson et al.

* Corresponding author. Tel.: +91 4024443169; fax: +91 4024442699.
E-mail addresses: royjohnson@arci.res.in, hareesh@arci.res.in (R. Johnson).

0272-8842/$36.00
doi:10.1016/j.ceramint.2011.05.151

investigated the relationship between YSZ sample density and its corresponding ionic conductivity [10]. Approaches to lower the operating temperature of SOFC resulted in the emergence of compounds such as doped ceria and LSGM as intermediate/low temperature electrolyte materials. Further reducing the electrolyte thickness in anode-supported solid oxide fuel cells (SOFCs) had also aided in reducing the operational temperature. Nevertheless, the use of such materials in place of the conventional YSZ electrolyte is met with problems associated with the stability of these materials under harsh operating environments, such as low mechanical strength and stability in addition to the poor chemical compatibility with cathode materials. Hence 8YSZ is still the candidate electrolyte material for SOFC's applications by virtue of high chemical and thermal stability, excellent mechanical properties and pure ionic conductivity over a wide range of operating conditions.

In recent years, considerable efforts were made in reducing the sintered grain size of electrolytes down to the nano-scale in order to enhance the ionic conductivity. Nano-crystallinity introduces such a high density in the interfaces that the conduction properties may become interface-controlled [11]. Han et al. [12] reported a higher ionic conductivity for 8YSZ electrolytes with a smaller grain size and the lower thickness of the intergranular regions. Li et al. [13] have attributed higher resistance of the grain boundaries to the impurity phase.

Processing methods and conditions can also greatly influence the conductivity of electrolytes and importantly the sintering methodology employed for microstructural control and densification play a major role. Kleitz et al. [14] and Dessemond et al. [15] observed high values of grain boundary resistance at low relative density of the electrolyte sintered at low sintering temperatures and a linear correlation between grain boundary conductivity and porosity of the sintered electrolyte. Near theoretical density with fine grained microstructure is therefore an essential prerequisite for a high-performing ionic conductor.

In the present study 8 mol% yttria-stabilized zirconia (8YSZ) ceramics was sintered to >99% of theoretical density under the techniques of conventional ramp and hold (CRH) and two-stage sintering (TSS). Additionally non conventional sintering techniques such as spark plasma sintering (SPS) and microwave sintering (MWS) were also employed for densification studies. In SPS technique, samples were sintered at temperatures of 1325 °C and 1425 °C (to intentionally grow the grain) elucidate the effect of sintered grain sizes on ionic conductivity of 8YSZ. A comparative study on microstructure evolution and grain boundary, grain interior conductivities were carried out for samples obtained by all the attempted sintering techniques. Attempts are also made to explain the highest conductivity exhibited by SPS sintered samples.

2. Experimental procedure

2.1. Slip casting of specimens

Commercially available zirconia powder (TZ-8Y, Tosoh, Tokyo, Japan) was subjected to XRD (D8 Advanced, Bruker AXS, Karlsruhe, Germany) for phase characterization and morphological studies by SEM (HITACHI S-3400N, Tokyo, Japan). The powder was dispersed in aqueous medium using 1 wt% Darvan 821A (R.T. Vanderbilt Co., Inc., Norwalk, CT, USA) as dispersant and octanol (Merck, India) was used as the antifoaming agent to form slurries having solid loading in the range of 55–65 wt%. The slurries, optimized with respect to their solid loading based on their rheological properties were then cast into square discs of 12 mm × 12 mm size in Plaster of Paris moulds followed by drying under controlled humidity conditions of 50 °C and 75% RH.

2.2. Sintering methodologies

Under the category of conventional sintering methodologies, specimens were sintered by the sintering techniques of conventional ramp and hold (CRH) and two stage sintering (TSS). In CRH methodology, the specimens were sintered in a PID controlled laboratory furnace (Nabertherm R, Model: HT 64/17, Bremen, Germany) at 1525 °C for 2 h at a heating rate of 5 °C/min. In TSS methodology the specimens were first heat treated to a temperature of 1525 °C followed by a second step hold at the lower temperature of 1350 °C for 4 h. Under non-conventional sintering methodologies, the specimens were sintered by SPS (Dr. Sinter 1050, SPS Syntex Inc., Kanagawa, Japan) with a heating rate of 170 °C/min to peak temperatures of 1325 °C with a holding time of 5 min. Microwave sintering was carried out (Linn High Therm MHTD 1800-6, 4/2, 45 with 2.45 GHz frequency, Linn High Therm GmbH, Eschenfelden, Germany) at a heating rate of 10 °C/min to peak temperatures of 1525 °C with a holding time of 15 min.

The sintered specimens were characterized for their density using Archimedes principle and microstructural analysis of polished and thermally etched specimens were carried out using Field Emission Scanning Electron Microscope (HITACHI S-4300SC/N, Tokyo, Japan). Grain size analyses of the specimens were carried out by the linear intercept method. The impedance spectroscopy measurements were carried out using an Impedance analyzer (Solartron SI1260, Ametek, Inc., Hampshire, UK) in the frequency range varying from 0.1 Hz to 10 MHz and applied ac amplitude of 100 mV. To measure the ionic conductivity, the samples were first coated with silver paste on both sides of the electrolyte as electrodes, and fired at 550 °C for 15 min. In the study of temperature response, the samples were placed in a Probostat made sample holder and impedance was measured between 300 °C and 800 °C at 50 °C increments with a computer aided data acquisition system.

3. Results and discussion

3.1. Sintering methodologies and microstructural analysis

Fig. 1(a) and (b) shows the X-ray diffraction pattern and powder morphology of 8YSZ powder. All the peaks of XRD pattern correspond to the fluorite structure of ZrO_2 and are characteristic of the cubic phase of powder. SEM micrographs

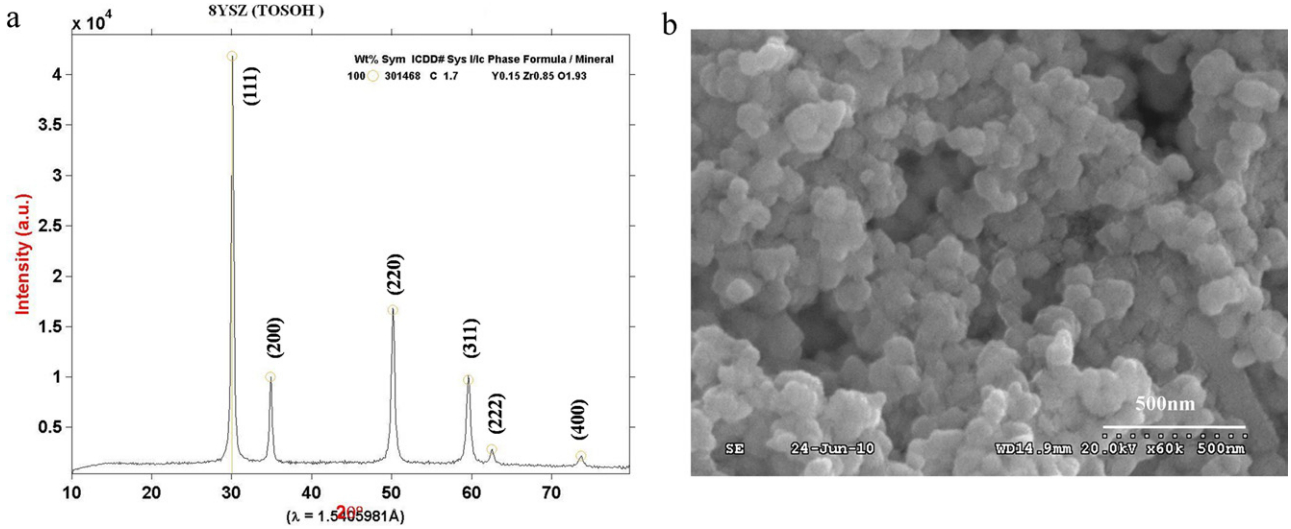

Fig. 1. (a) and (b) XRD pattern and powder morphology of 8YSZ powder showing Cubic Structure as a major phase due to full stabilization and uniform particle size.

Table 1
Sintering parameters, sintered densities and average grain sizes of CRH, TSS, MWS and SPS specimens.

Specimen identity	Sintering technique	Sintering temperature (°C)	Dwell time	Density (g/cm^3)	% Theoretical density	Average grain size (μm)
I	CRH	1525	2 h	5.867	99.44	4.67
II	TSS	T1:1525 T2:1350	5 min 4 h	5.865	99.40	2.64
III	MWS	1525	15 min	5.850	99.15	3.70
IV	SPS	1325	5 min	5.870	99.50	1.16
V	SPS	1425	5 min	5.870	99.50	8.8

exhibited a spherical morphology with the mean particle size of around 90 nm.

Table 1 presents the sintering parameters, densities and sintered grain sizes of zirconia samples densified using the sintering methodologies of CRH, TSS, MWS and SPS. In CRH mode the samples could be sintered to densities >99%TD in the temperature range of 1500–1525 °C. When the methodology is modified as per TSS technique selecting a peak temperature of 1525 °C, zirconia samples densified to >99%TD at a lower soaking temperature of 1350 °C. In MWS, the temperature regime for good densification (>99%TD) matched that of the CRH mode (1500–1550 °C) but at substantially low soaking periods of 15 min compared to 2 h in CRH. Maximum densification at the lowest sintering temperature was provided by SPS wherein samples could be sintered to >99%TD at a temperature of 1325 °C for 5 min, which is higher than the reported values [16].

Fig. 2(a) presents the SEM microstructure of 8YSZ samples sintered by CRH at 1525 °C. Average grain size measurement by linear intercept method provided a value around 4.6 μm. 8YSZ sample sintered by the TSS technique at the lower soaking temperature of 1350 °C indicates relatively finer microstructure with few scattered inter-granular pores (Fig. 2(b)). The grains are of uniform sizes averaging around 2.5 μm. The significant decrease in grain size during the TSS can be attributed to the fact that the first heating step to high temperature of 1550 °C for a shorter duration closes the porosity and the second step hold at 1350 °C, the lower temperature, for a longer period of time imparts densification with limited grain growth.

During MW sintering, samples achieved 99%TD at 1525 °C and are similar to the values attained during CRH. The MWS sample exhibited the grain sizes marginally lower than that of CRH (3.6 μm compared to 4.6 μm in CRH) at nearly identical density values, primarily due to shorter soaking times. During microwave heating energy is transferred to the material electromagnetically and not as a thermal heat flux enabling the material to be heated at rapid rates [17]. The higher oxygen vacancies associated with 8 mol% yttria stabilized zirconia provides higher ionic conductivity at elevated temperatures leading to high dielectric losses and enhanced absorption of microwaves. This mechanism could be one possible reason for the shorter sintering times in MWS. Microstructure presented in Fig. 2(c) represents that of a dense sample with very few inter-granular pores. Grain growth with temperature was prominent without appreciable density changes during the increase of temperature from 1525 °C to 1550 °C.

The microstructures of SPS sintered specimens at 1325 °C and 1425 °C are provided in Fig. 2(d) and (e). Dense microstructure with extremely fine grain sizes was observed and the average grain size was found to be ~1 μm in 1325 °C sintered sample, which is 5 times lower in magnitude than the reported in Ref. [16]. A significant increase in grain size to 8.8 μm was observed in 1425 °C SPS sample. The particle size to sintered grain size ratio is quite low (a factor of 5) at 1325 °C

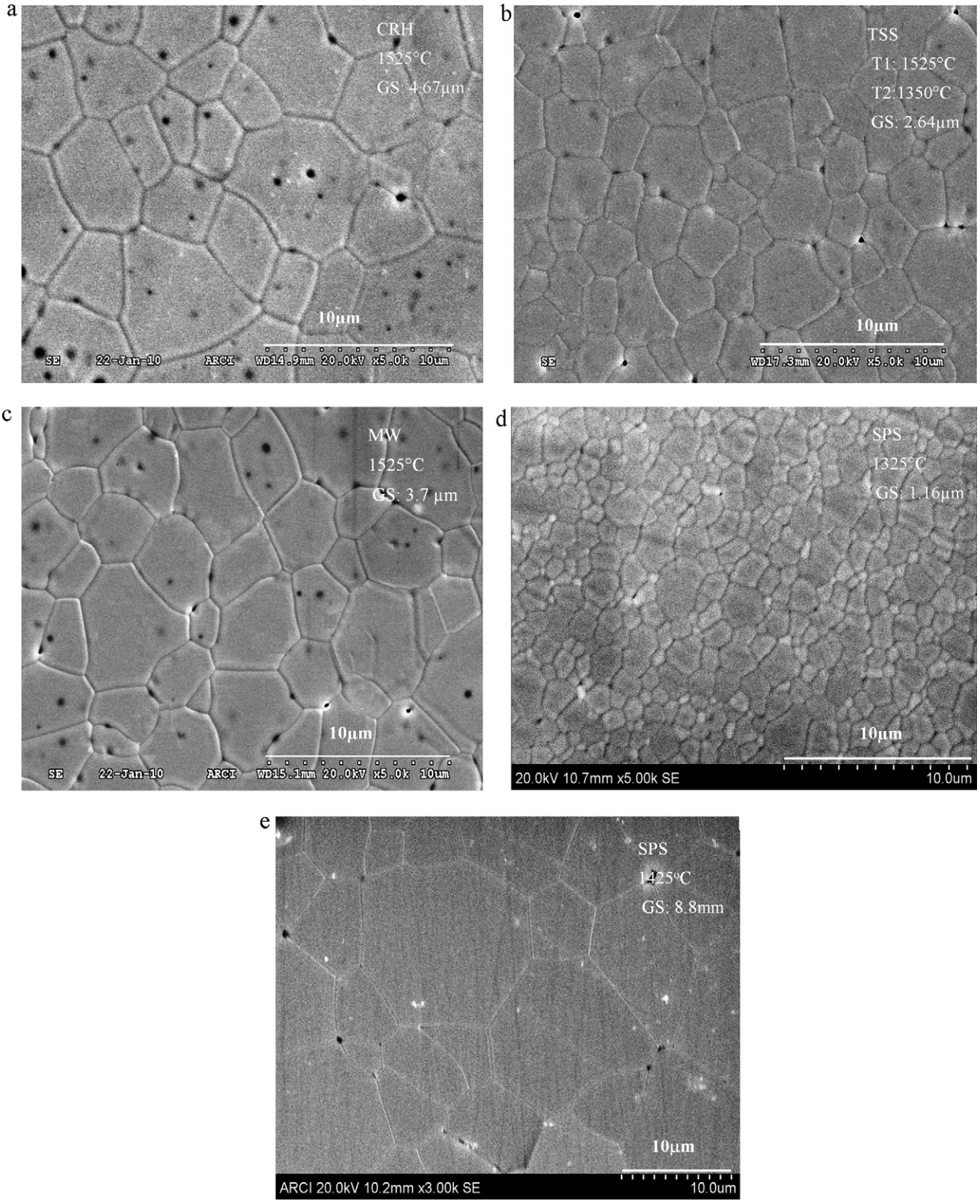

Fig. 2. A comparison of the microstructure of sintered 8YSZ specimens (>99%TD) of (a) CRH-1525 °C; (b) TSS-T1: 1525 °C, T2: 1350 °C; (c) MWS-1525 °C; (d) SPS-1325 °C and (e) SPS-1425 °C.

compared to the other sintering techniques employed. However, the particle size to sintered grain size increased by a factor of 8 in 1425 °C SPS sintered sample, indicating the importance of selection of SPS sintering temperatures.

Low temperature densification supplemented by rapid sintering rates by SPS depresses the grain growth of polycrystals. When the consolidation is completed in few minutes, including heating and holding cycles, the grains could

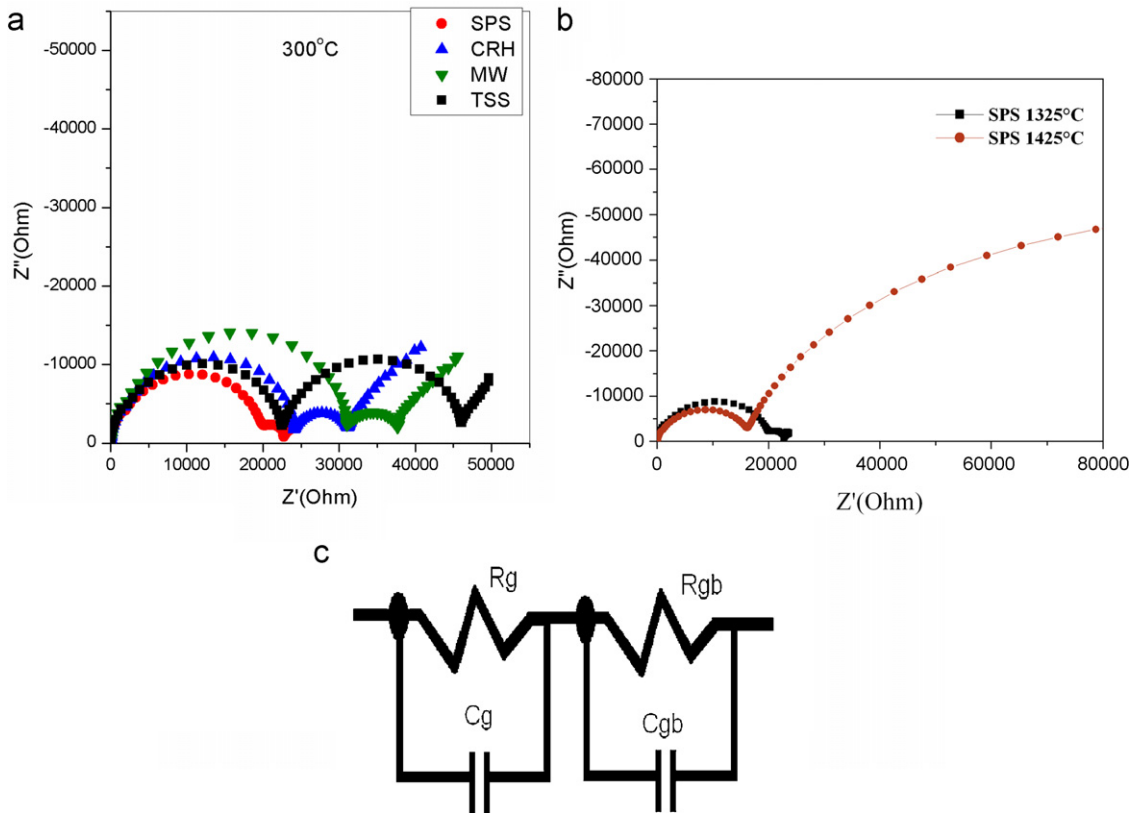

Fig. 3. (a) Complex impedance plane plots of CRH, TSS, MWS and SPS specimens at 300 °C; (b) Cole–Cole plots of SPS samples sintered at 1325 and 1425 °C; (c) equivalent circuit of SPS sample.

be small. The rapid densification of samples by SPS is attributed to mechanisms like particle rearrangement and breaking up of agglomerates aided by the applied pressure and faster heating rates [18]. By rearrangement of particles, the SPS process also suppresses the increase in pore size generally observed during the first and intermediate stages of sintering thereby facilitating the sintering process. Further, applied electric field promotes the diffusion of ions and vacancies and in turn accelerates the densification process.

The grain growth is a result of grain boundary diffusion and grain boundary migration. At low temperatures, grain boundary diffusion continues and at elevated temperatures, grain boundary migration dominates for grain growth [19]. Grain boundary migration needs higher activation energy than grain boundary diffusion. The feasibility of densification without grain growth relies on the suppression of grain boundary migration, while keeping grain boundary diffusion active. Decreasing the sintering temperature to 1250–1350 °C, can suppress grain boundary migration without any affect to grain boundary diffusion, and as a result the size of YSZ grains stay within a definite range [1]. In this way, the size of YSZ grain does not increase dramatically and the pores gradually disappear by grain boundary diffusion resulting in dense ceramic bodies with finer grain sizes, as has been found in 8YSZ samples sintered through SPS technique.

3.2. Ionic conductivity

A typical complex impedance plane plots, Z' vs. Z'', recorded at the temperature of 300 °C for the CRH, TSS, MWS and SPS samples are shown in Fig. 3(a). The plots show semicircles in all the samples and the contribution of grain interior and grain boundaries can be distinguished clearly. The curve observed in the low frequency region corresponds to electrolyte/electrode interface. It is clear that there is a difference in the diameter of the high and mid frequency semicircles (grain/grain boundary resistance) among the samples processed through different sintering routes, indicating a different rate of oxygen ion migration due to difference in grain sizes and grain boundary area.

Out of the four samples subjected to impedance analysis, SPS sample has shown low grain and grain boundary resistances (Fig. 3(a)). At 300 °C, the grain boundary resistivity of SPS sample sintered at 1325 °C is 1.3×10^4 Ω-cm, while the SPS sample sintered at 1425 °C had shown value of 6.11×10^5 Ω-cm (Fig. 3(b)). The total resistivity of SPS sample sintered at 1325 °C as evidenced by the plot is significantly lower, when compared to TSS, CRH and MWS samples where the values are in the order of 3×10^5 Ω-cm. The impedance spectra indicate that the grain boundary resistivity is extremely small in SPS sample. It can be inferred that YSZ electrolyte prepared by spark plasma sintering process is

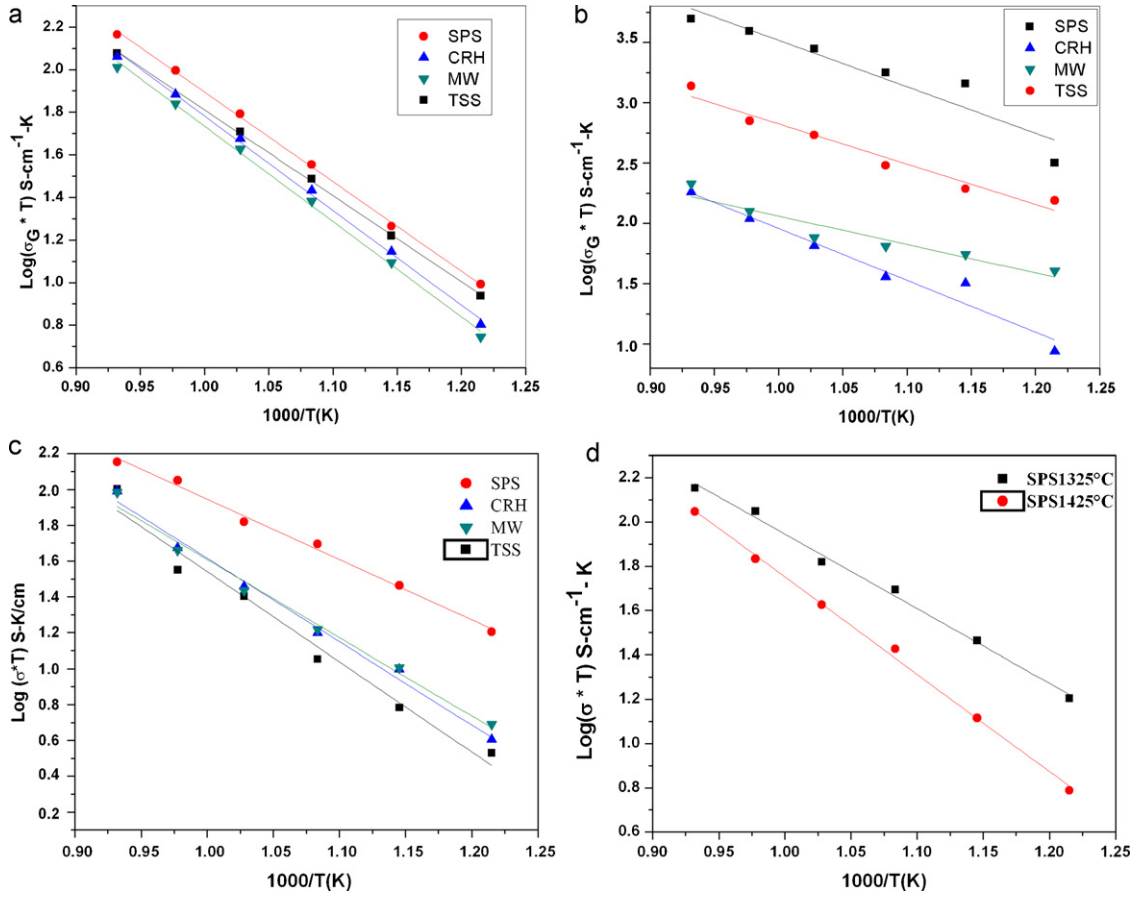

Fig. 4. (a)–(c) Arrhenius plots for the grain, grain boundary and total conduction of 8YSZ samples of different sintering techniques; (d) Arrhenius plots for 8YSZ sintered by SPS at 1325 °C and 1425 °C.

favorable to improve electrical conductivity. Further with the increase of temperature, the grain and grain boundary resistivities decreased in all the samples tested under the present study. Though grain boundary resistivity (R_{gb}) is smaller than grain resistivity (R_g) in the temperature regime where SOFC works actually, R_{gb} is competitive with R_g. However, the ionic conductivity in the boundary would be very small compared with that of the bulk, if the volume fraction of the boundary was considerably small as approximated in the literature [20]. Therefore, improvement of boundary ionic conductivity is very important for the development of SOFC electrolytes.

Highest ionic conductivity of 0.134 S/cm at 800 °C is exhibited by SPS sample sintered at 1325 °C with grain size of 1.16 μm with a decrease in conductivity to 0.104 S/cm for SPS sample sintered at 1425 °C with a grain size of 8.8 μm. The conductivity of 1325 °C SPS sample in the present study exhibited a relatively higher value in comparison to the 0.105 S/cm reported by Chen et al. [21] and 0.118 S/cm reported by Zha et al. [22] in earlier studies. Ionic conductivity of all the samples sintered through all other sintering techniques such as TSS, CRH and MWS was found to be in the range of ∼0.09 S/cm which is close to the conductivity of 8YSZ ceramics reported earlier [8,23].

Dahl et al. [24] reported relatively low ionic conductivity of spark plasma sintered 8YSZ around 0.082 S/cm at 900 °C even with the smaller average grain size of 210 nm in comparison to the presently reported value of 0.134 S/cm. This can be attributed to the high density value of >99% of TD achieved through SPS sintering parameters in the present study in comparison to the 96% reported by the above study. Prabhakaran et al. [25] showed the ionic conductivity of 0.130 S/cm at 1000 °C for 8YSZ conventionally sintered specimens with average grain size of 1.4 μm and density of 97% of TD. Further, Hesabi et al. [26] also reported ionic conductivity values of 0.132 S/cm at 900 °C for two step sintered specimens with average grain size of 0.9 μm and density of 98% TD. The present study demonstrates the ionic conductivity values in the close ranges of above reported studies at a relatively low temperature of 800 °C due to the optimized SPS sintering parameters and the unique sintering mechanisms leading to the high densification at low temperatures with fine grained microstructures.

Fig. 3(c) shows the equivalent circuit for 8YSZ electrolyte. It is composed of two parallel RC circuits, where the resistance R_g is denotes as the grain resistance and R_{gb} grain boundary resistance. The corresponding capacitances of grain and grain boundary are C_g and C_{gb}. Grain and grain boundary conductivities were calculated from the Cole–Cole plots at various temperatures for the CRH and MWS, TSS and SPS samples and plotted against the operating temperature regime as shown in Fig. 4(a)–(d). Further, activation energies of total

bulk conductivity for various samples were calculated by fitting the data to the Arrhenius relation for thermally activated conduction which is given as:

$$\sigma = \frac{\sigma_o}{T} \exp\left(\frac{-E_a}{kT}\right) \quad (1)$$

where E_a is the activation energy for conduction, T the absolute temperature, K the Boltzmann's constant and σ_o the pre-exponential factor. The linear fit is applied for the conductivity data using least square fitting technique. The activation energies were found to be lower (0.68 eV) for SPS, as expected, in comparison to 0.79 eV, 0.71 eV and 0.99 eV for CRH, MWS and TSS samples respectively. Thus sintering methodology affects conductivity and activation energy. As all the specimens are densified to >99% of the theoretical density, the resistance offered by the grain boundary becomes critical and is determined by its area and the oxygen ion concentration. It is well known that the general grain conductivity is higher by two to three times than the grain boundary conductivity.

The influence of the grain boundary conductivity in the total conductivity can be evaluated through the blocking factor (α_R) [27,28] defined from the impedance diagram parameters by:

$$\alpha_R = \frac{R_{gb}}{(R_g + R_{gb})} \quad (2)$$

where R_g and R_{gb} are grain and grain boundary resistivities respectively. This factor gives the fraction of the electric carriers being blocked at the impermeable internal surfaces, under the measuring conditions, with respect to the total number of electric carriers in the sample. Table 2 shows the blocking factor as a function of temperature for all compositions. The lowest blocking factor was observed in SPS sample for all ranges of temperature. The assumption that the observed blocking effect in stabilized zirconia results directly from the formation of blocked zones, where electric carriers are trapped and do not contribute to the transport of electric current. These results suggest that the SPS promotes grain boundary conduction and hence the total conduction in 8YSZ [29].

Table 2
Blocking factor (α) measured at 800 °C for 8YSZ samples sintered through different sintering methods.

Sample	a_{800} (°C)
CRH	0.38
TSS	0.33
MW	0.32
SPS-1325 °C	0.26
SPS-1425 °C	0.29

The high bulk ionic conductivity of SPS sintered sample in the present study can be attributed to the decrease in grain and grain boundary resistances resulting from the lower blocking factor (α) of 0.26–0.29 measured at 800 °C. Earlier studies attributed the lower grain boundary conductivity to the segregation of a blocking layer with space charges for oxygen ion conduction and decrease of oxygen ion conduction when the oxygen vacancy concentration at the grain boundary becomes lower than that in the grain interior [30,31].

It is evident from the microstructures of the samples that except in SPS, the samples sintered through CRH, TSS and MWS, indicated black spots distributed along the grains and grain boundaries. EDS analysis of these samples at various spots is carried out. A typical analysis of CRH and SPS samples is depicted in Fig. 5(a) and (b). The black spots (Fig. 5(a)) in the microstructure reveals yttria segregation arising out of exposure to highly sintering temperatures of $T > 1500$ °C which was necessary to achieve the density requirements of >99%TD in case of CRH, TSS and MW sintered samples. As a consequence of this selective segregation of Y_2O_3, there is a non uniform distribution on a microstructural scale leading to depletion in oxygen vacancies and hence a drop in oxygen ion transport.

Unlike other techniques, SPS technique achieved a density of >99% at significantly lower sintering temperatures of 1325 °C and 1425 °C. There is no evidence of yttria segregation as the microstructure is devoid of black spots in SEM imaging as was confirmed also from EDS analysis (Fig. 5(b)). It can further be observed from EDS analysis (Fig. 5(a)) that SPS samples are characterized by a uniform distribution of yttria

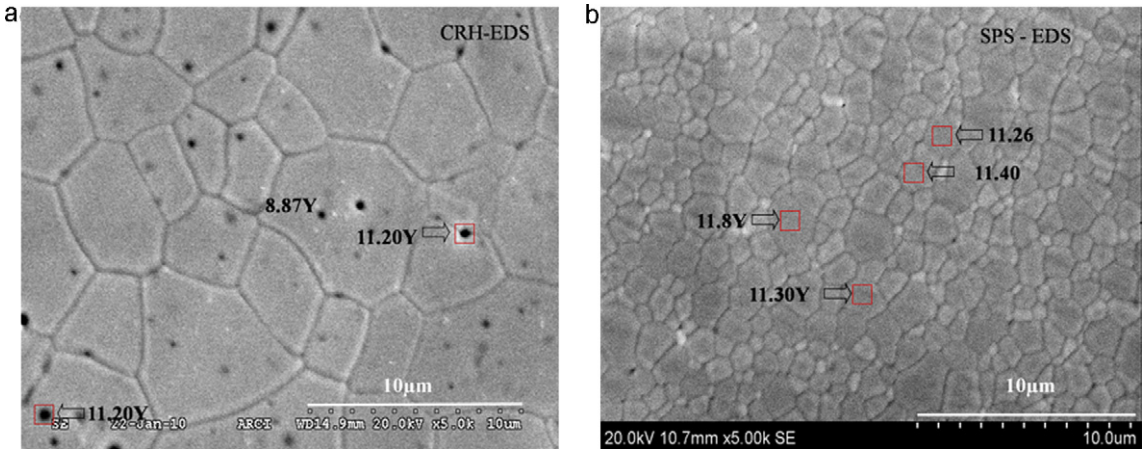

Fig. 5. (a) and (b) EDS analysis showing the distribution of yttrium for CRH and SPS samples.

with negligible variation of yttria content in wt% (12.38–12.49) as against 13.8 wt% in fully stabilized zirconia. This can be attributed to the unique sintering mechanisms operative in SPS technique enabling low temperature densification at temperatures of 1325 °C. The results of the present study suggest that with enhancement of the ionic conductivity through grain refining and lowering the sintering temperature using SPS method, working temperature of the electrolyte could be lowered.

4. Conclusions

8 mol% yttria stabilized zirconia specimens were densified to >99% of theoretical density through optimized sintering parameters employing various sintering techniques such as conventional ramp and hold (CRH), two-stage sintering (TSS), microwave sintering (MWS) and spark plasma sintering (SPS).

A substantial variation in grain sizes was observed based on the sintering methodologies with highest average grain size of 4.67 μm observed for CRH followed by 3.70 μm for MWS, 2.64 μm for TSS and 1.16 μm for SPS technique which can be well correlated with the underlying sintering mechanisms operative in each technique.

Out of the CRH, MWS, TSS and SPS samples subjected to impedance analysis, SPS sample has shown low grain and grain boundary resistances at all measured temperature regimes and accordingly the bulk conductivity of SPS sample (0.134 S/cm) was found much higher than TSS, CRH and MWS, samples which was in the range of ∼0.09 S/cm. Further the blocking factor calculated was also found to be lowest 0.26 for the SPS sintered sample confirming the above observation.

Microstructural and EDS analysis revealed yttria segregation due to high temperature exposure ($T > 1500$ °C) of samples by CRH, TSS and MWS techniques. The selective segregation of Y_2O_3 leads to depletion in oxygen vacancies resulting in decrease of oxygen ion transport. However, no evidence of segregation is observed with SPS sintered samples due to its unique sintering mechanisms facilitating low temperature densification at 1325 °C.

References

[1] I.W. Chen, X.H. Wang, Sintering dense nano-crystalline ceramics without final stage grain growth, Nature 404 (2000) 168–171.

[2] P.C. Yu, Q.F.,Q.F. Li, J.Y.H. Fuh, T. Li, L. Lu, Two-stage sintering of nano-sized yttria stabilized zirconia process by powder injection molding, J. Mater. Proc. Technol. 192–193 (2007) 312–318.

[3] G. Bernard-Granger, C. Guizard, Spark plasma sintering of a commercially available granulated zirconia powder: 1. sintering path and hypotheses about the mechanism(s) controlling densification, Acta Mater. 55 (2007) 3493–3504.

[4] U. Anselmi-Tamburini, J.E. Garay, Z.A. Munir, Fast low-temperature consolidation of bulk nanometric ceramic materials, Scripta Mater. 54 (5) (2006) 823–828.

[5] M.G. Bellino, D.G. Lamas, N.E. Walsöe de Reca, Enhanced ionic conductivity in nanostructured heavily doped ceria ceramics, Adv. Func. Mater. 16 (1) (2006) 107–113.

[6] P. Dahl, I. Kaus, Z. Zhao, M. Johnsson, M. Nygren, K. Wiik, T. Grande, M.A. Einarsrud, Densification and properties of zirconia prepared by three different sintering techniques, Ceram. Int. 33 (8) (2007) 1603–1610.

[7] Z. Shen, Z. Zhao, H. Peng, M. Nygren, Formation of touch interlocking microstructures in silicon nitride ceramics by dynamic ripening, Nature 417 (2002) 266–269.

[8] N.Q. Minh, Ceramic fuel cells, J. Am. Ceram. Soc. 76 (1993) 563–588.

[9] S.P.S. Badwal, Zirconia-based solid electrolytes: microstructure, stability and ionic conductivity, Solid State Ion. 52 (1992) 23–32.

[10] I.R. Gibson, G.P. Dransfield, J.T.S. Irvine, Sinterability of commercial 8 mol% yttria stabilized zirconia powders and the effect of sintered density on the ionic conductivity, J. Mater. Sci. 33 (1998) 4297–4305.

[11] J. Maier, Ionic transport in nano-sized systems, Solid State Ion. 175 (2004) 7.

[12] M. Han, X. Tang, H. Yin, S. Peng, Fabrication, microstructure and properties of a YSZ electrolyte for SOFCs, J. Power Sources 165 (2007) 757–763.

[13] Q. Li, T. Xia, X.D. Liu, X.F. Ma, M. Meng, X.Q. Cao, Fast densification and electrical conductivity of yttria-stabilized zirconia nano ceramics, Mater. Sci. Eng. B 138 (2007) 78–83.

[14] M. Kleitz, C. Pescher, L. Dessemond, in: S.P.S. Badwal, M.J. Bannister, R.H.J. Hannink (Eds.), Science and Technology of Zirconia V, Technomic, Lancaster, PA, 1993, p. 593.

[15] L. Dessemond, J. Guindet, A. Hammou, M. Klerta, in: F. Grosz, P. Zegers, S.C. Singhal, O. Yamamoto (Eds.), Proceedings of the 2nd International Symposium on SOFCs, Brussels, Belgium, (1991), p. 409.

[16] X.J. Chen, K.A. Khor, S.H. Chan, L.G. Yu, Overcoming the effect of contaminant in solid oxide fuel cell (SOFC) electrolyte: spark plasm sintering (SPS) of 0.5 wt% silica-doped yttria-stabilized zirconia (YSZ), Mater. Sci. Eng. A 374 (2004) 64–71.

[17] W.H. Sutton, Microwave processing of ceramic materials, Am. Ceram. Soc. Bull. 68 (1989) 376–386.

[18] T. Takeuchi, M. Tabuchi, I. Kondoh, N. Tamari, H. Kageyama, Synthesis of dense lead zirconate titanate ceramics with sub-micrometer grains by spark plasma sintering, J. Am. Ceram. Soc. 83 (2000) 541–544.

[19] M.P. Harmer, R.J. Brook, Fast firing-microstructural benefits, J. Brit. Ceram. Soc. 80 (1980) 147–149.

[20] E. Iguchi, K. Ueda, W.H. Jung, Conduction in $LaCoO_3$ by small-polaron hopping below room temperature, Phys. Rev. B 54 (1996) 17431.

[21] X.J. Chen, K.A. Khor, S.H. Chan, L.G. Yu, Influence of microstructure on the ionic conductivity of yttria-stabilized zirconia electrolyte, Mater. Sci. Eng. A 335 (2002) 246–252.

[22] S. Zha, C. Xia, G. Meng, Effect of Gd(sm) doping on properties of ceria electrolyte for solid oxide fuel cells, J. Power Sources 115 (2003) 44.

[23] D.S. Patil, K. Prabhakaran, Rajiv Dayal, C. Durga Prasad, N.M. Gokhale, A.B. Samui, S.C. Sharma, Eight mole percent yttria stabilized zirconia powders by organic precursor route, Ceram. Int. 34 (2008) 1195–1199.

[24] P. Dahl, I. Kaus, Z. Zhao, M. Johnson, M. Nygren, K. Wiik, T. Grande, M.-A. Einarsrud, Densification and properties of zirconia prepared by three different sintering techniques, Ceram. Int. 33 (2007) 1603–1610.

[25] K. Prabhakaran, M.O. Beigh, J. Lakra, N.M. Gokhale, S.C. Sharma, Characteristics of 8 mol% yttria stabilized zirconia powder prepared by spray drying process, J. Mater. Proc. Technol. 189 (2007) 178–181.

[26] Z. Razavi Hesabi, T. Mehdi Mazaheri, Ebadzadeh, Enhanced electrical conductivity of ultrafine-grained $8Y_2O_3$ stabilized ZrO_2 produced by two step sintering technique, J. Alloys Compd. 494 (2010) 362–365.

[27] R. Gerhardt, A.S. Nowick, Grain boundary effect in ceria doped with trivalent cations: I, electrical measurement, J. Am. Ceram. Soc. 69 (9) (1986) 641–646.

[28] M.J. Verkerk, B.J. Middlehuis, A.J. Burggraaf, Effect of grain boundaries on the conductivity of high purity ZrO_2–Y_2O_3 ceramics, Solid State Ion. 6 (1982) 159.

[29] X.J. Chen, K.A. Khor, S.H. Chan, L.G. Yu, Preparation of yttria-stabilized zirconia electrolyte by spark-plasma sintering, Mater. Sci. Eng. A 341 (2003) 43–48.

[30] Waser, in: N. Setter, E.L. Colla (Eds.), Ferroelectric Ceramics, Monte Verita, Birkhauser, Basel, 1993.

[31] B. Liu, Y. Zhang, LSGM sintered by spark plasma sintering (SPS) for intermediate temperature SOFC electrolyte, J. Alloys Compd. 458 (2008) 383–389.